

A Frequency Tunable Dielectric Resonator Antenna with Reduction of Cross Polarisation for Wi-MAX and Sub-6 GHz 5G Applications

Rajkishor Kumar^{#,*}, Avinash Chandra[#], Naveen Mishra[#] and Raghvendra Kumar Chaudhary[§]

[#]*School of Electronics Engineering, Vellore Institute of Technology, Vellore - 632 014, India*

[§]*Department of Electrical Engineering, Indian Institute of Technology, Kanpur - 208 016, India*

^{*}*E-mail: rajkishorkumar88@gmail.com*

ABSTRACT

A frequency Tunable (mechanical tuning) Linearly Polarized (TLP) rectangular Dielectric Resonator Antenna (DRA) coupled with a horizontal/vertical-slot and excited with circular-ring type feed is investigated in this article. The frequency tunability (mechanical tuning) is achieved by the rotation of slot at different angles of the proposed structure. Hence, two linearly polarized antennas have been proposed for different frequency bands such as Wi-MAX and Sub-6 GHz/5G, respectively, using slot variations (named as DRA-1 and DRA-2). TE_{116} mode has been excited in both the DRAs and confirmed by orientation of electric field inside the rectangular DRA. The measured -10 dB input impedance bandwidths of DRA-1 offer 21.60 % being centered at 2.87 GHz and the separation of co-polarized and cross-polarized field levels is above -24 dB in the broadside direction (xz -plane). Whereas DRA-2 offers measured -10 dB input impedance bandwidths of 23.03% being centered at 3.56 GHz having a separation of co-polarized and cross-polarized field levels are above -23 dB in the broadside direction (xz -plane). In addition, the proposed DRA-1 and DRA-2 show a maximum gain of 5.23 dBi and 4.75 dBi in broadside direction, respectively.

Keywords: Frequency tunable; Dielectric resonator antenna; Slot coupled; Sub-6 GHz; 5G applications

1. INTRODUCTION

Dielectric resonator antennas (DRAs) offer many advantages like increasing antenna impedance bandwidth, radiation efficiency and gain because; there are no metallic and surface wave losses¹. DRAs have different types of shapes like hemispherical, cylindrical, and rectangular, respectively which are supported by theoretical and mathematical derivations to find out all the components²⁻⁵. It also have ease of excitations such as coaxial probe, microstrip, aperture/ slot coupling, conformal and CPW fed, respectively, which are also validated by theoretical and mathematical derivations to find out the most probable coupling between the DRA and feeding mechanisms^{1,6}. The compact size and low profile is the another advantages of the DRAs⁷. Linearly polarized (LP) antennas are one of the key device for modern wireless communication applications like radar and satellite communication because of stable near-and far-field characteristics⁸.

To suppress the cross polarization, the aperture or slot coupling are more frequently used by the various researches because of it have mathematical and theoretical backup to calculate the initial values of slot length, width and stub size, respectively. By controlling all slot parameters along with slightly shifting the position of DRA shows the desired coupling of the various applications^{1,9-11}.

In the current scenario, the requirement of bandwidth is increases abnormally due to increases number of users.

Therefore, researchers are trying to increase the bandwidth of DRA by using suitable feeding techniques (simple/ complex) and modified the shape of dielectric resonators (DRs)¹²⁻¹³. The deformations shapes of DRs are one of the options for increasing the bandwidth but it is very complicated and challenging to make such types of shapes¹⁴⁻¹⁷.

Another option is the feeding mechanism because it also works as resonating structures; therefore together they produce a double resonating structure having identical radiation patterns. If the antenna designers required the wide bandwidth behaviours then by selecting the design of the DRA and feed, the two resonances can be combined to achieve wide bandwidth otherwise it will give two resonances at different frequency of operations¹⁸⁻¹⁹. However, to avoid this complexity, researcher proposed conventional shape of DR with suitable feeding techniques to enhance the bandwidth²⁰⁻³⁰. There are mainly three methods reported in literature to achieve the tunability conditions such as tunable materials, mechanical actuation and electronic devices, respectively³¹. Some of the researchers were used the multiple parasitic strips³², bowtie slot³³, fluidic stub-loaded³⁴, and Mechanical Actuation³⁵ for getting the tunability conditions.

In this paper, a tuneable (mechanical tuning) linearly polarized rectangular DRA has been presented for Mid-Band 5G and Wi-MAX application bands. The presented radiator is coupled throughout a horizontal/vertical-slot and excited with circular-ring feed network for the generation of linearly polarized signal. Initially, DRA-1 has been designed by using horizontal slot (S_{L1}) which offers measured input impedance

bandwidth of 21.60 % (2.56-3.18 GHz) for Wi-MAX band applications (2.5-2.7 GHz). After that, the horizontal slot (S_{L1}) is replaced by vertical slot (S_{L2}) and named as DRA-2. This configuration shows measured input impedance bandwidth of 23.03 % (3.15-3.97 GHz) and it is used for Sub-6 GHz 5G applications (3.3-3.6 GHz). $TE_{11\delta}$ mode has been excited in both the proposed tuneable LP DRAs. Here, separate prototype antennas have been designed for the demonstrations of DRA-1 and DRA-2. The organization of proposed antenna is as follows: LP-1 DRA has been studied in section 2. Section 3 describes the LP-2 DRA configuration. Finally, conclusion is presented in section 4.

2. ANTENNA CONFIGURATIONS OF DRA-1 AND DRA-2

Figure 1 illustrates the shapes of presented DRA-1 and DRA-2. The rectangular DR is prepared from alumina (Al_2O_3), which consists of a dielectric constant and a loss tangent of 9.8 and 0.002, respectively. In both the configurations same rectangular DR is used with length D_L , width D_W and height D_H . Further, the same coupling of circular-ring feed was used in both configuration but the orientation of the slot in both configurations are different (i.e. DRA-1 uses a horizontal

whereas DRA-2 uses a vertical slot). A rectangular DR is placed on top of the ground plane, while a slot is printed in the ground plane and below that circular ring feed has been placed. The FR4 substrate has been used for separation between the ground plane and circular-ring feed with a dielectric constant and loss tangent of 4.4 and 0.025, respectively. The dimensions of FR4 substrate i.e., length, width and height, are S_L , S_W and S_H . The R_1 , R_2 and L_F , L_{F1} , W_F are represents the radius, lengths and width of circular-ring feed.

In theory, the resonance frequency of the lowest RDRA fundamental mode ($TE_{11\delta}$) is computed using the Dielectric Wave Guide Model (DWM) method²⁻⁵ for initial dimensions and Eqns are as follows:

$$k_x^2 + k_y^2 + k_z^2 = \epsilon_{dr} k_0^2 \tag{1}$$

$$k_x = m\pi/D_L, \quad k_y = n\pi/2D_H, \quad k_z = 2\pi/\lambda_0 \quad \text{where, } m = n = 1 \tag{2}$$

$$k_x * \tan\left(\frac{k_y D_x}{2}\right) = \sqrt{(\epsilon_{dr} - 1)k_0^2 - k_z^2} \tag{3}$$

$$f_0 = \frac{c}{2\pi\sqrt{\epsilon_{dr}}} * \sqrt{k_x^2 + k_y^2 + k_z^2} \tag{4}$$

Here, D_L , D_W and D_H denote the length, width, and height of the rectangular DRA; whereas ϵ_{dr} , c and k_0 denotes the

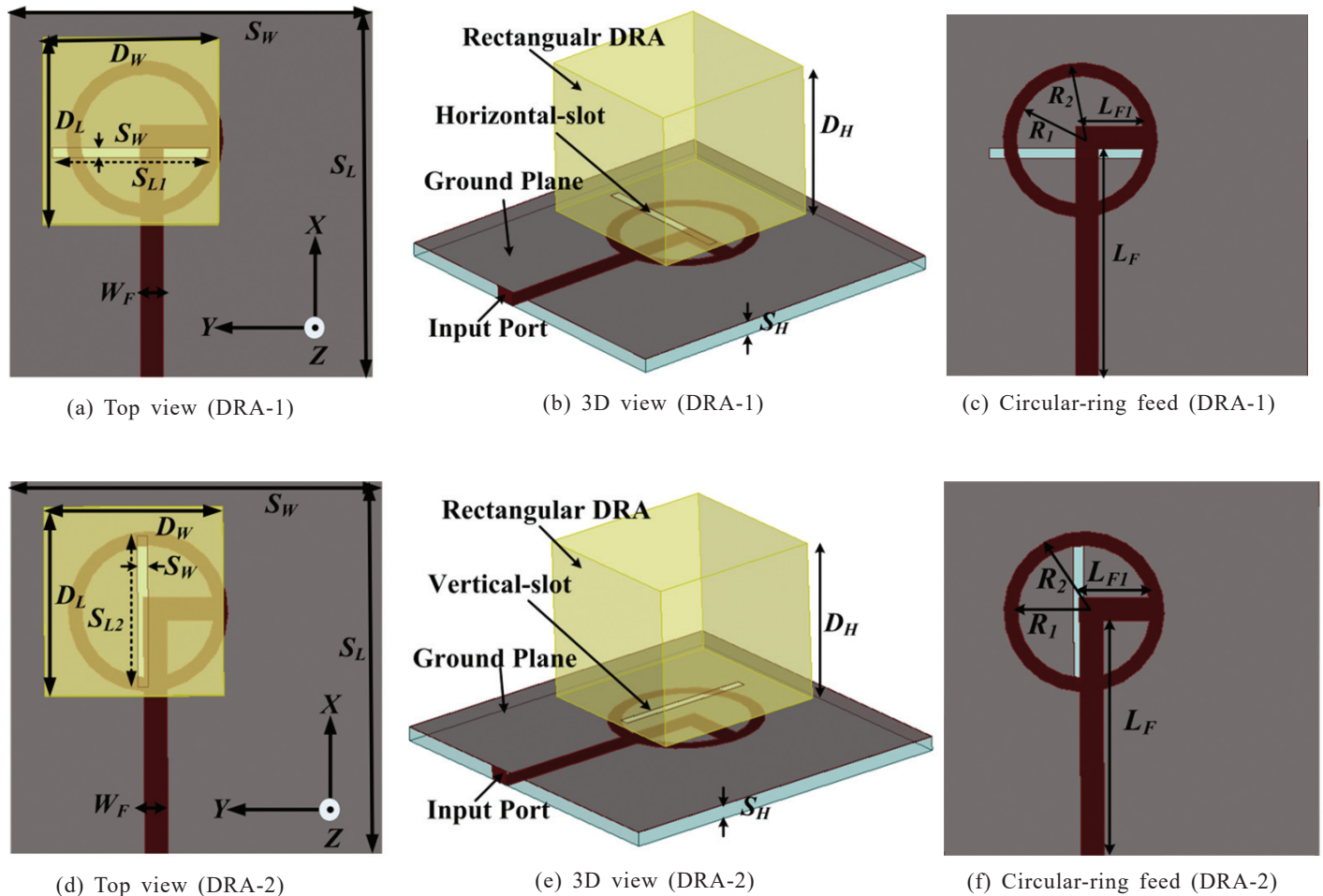


Figure 1. Schematic diagram of the proposed linearly polarized DRAs.

dielectric constant of dielectric resonator, speed of light and wavenumber in free space. The wave numbers in the x -, y - and z -directions were denoted as k_x , k_y and k_z inside the dielectric resonator respectively.

Using all initial DRA values, the computed resonance frequencies are obtained at about 2.85 GHz for DRA-1 and 3.55 GHz for DRA-2, respectively.

We were used the following guideline as a starting point for designing the rectangular slot, which are given below in equations wise and initial calculations are also provided.

- Here, the slot lengths (S_{L1} and S_{L2}) have been selected large enough so that the sufficient amount of coupling exists between the DR and feed line^{1, 9-11}
- $$S_{L1} = S_{L2} = \frac{0.4 \times \lambda_0}{\sqrt{\epsilon_{eff}}} \quad (5)$$

$$S_{L1} = \frac{0.4 \times \lambda_0}{\sqrt{\epsilon_{eff}}} = \frac{0.4 \times 97.08}{\sqrt{7.1}} = 14.57 \text{ mm} \quad (\lambda_0 \text{ for DRA - 1 is } 97.08 \text{ mm})$$

$$S_{L2} = \frac{0.4 \times \lambda_0}{\sqrt{\epsilon_{eff}}} = \frac{0.4 \times 91.46}{\sqrt{7.1}} = 13.71 \text{ mm} \quad (\lambda_0 \text{ for DRA - 2 is } 91.46 \text{ mm})$$

where, ϵ_{eff} is the effective permittivity of the DRA and substrate?

$$\epsilon_{eff} = \frac{\epsilon_{dra} \times \epsilon_{sub}}{2} \quad (6)$$

$$\epsilon_{eff} = \frac{\epsilon_{dra} \times \epsilon_{sub}}{2} = \frac{9.8 \times 4.4}{2} = 7.1$$

where, the dielectric constant for the dielectric resonator and the substrate is indicated by ϵ_{dra} and ϵ_{sub} , respectively.

- Next important parameter is slot width; the width of slot must be fairly narrow for avoiding the larger back lobe.

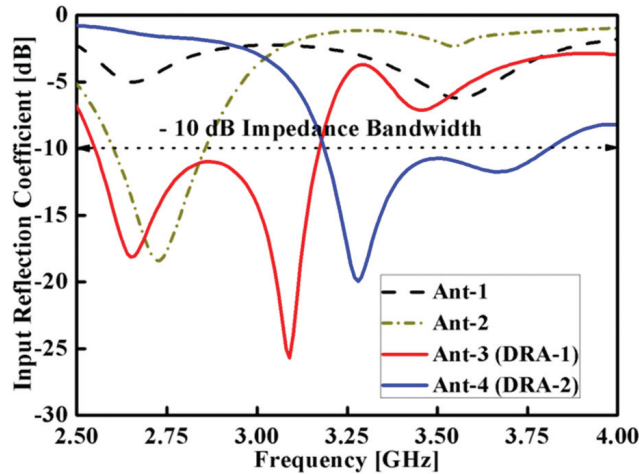
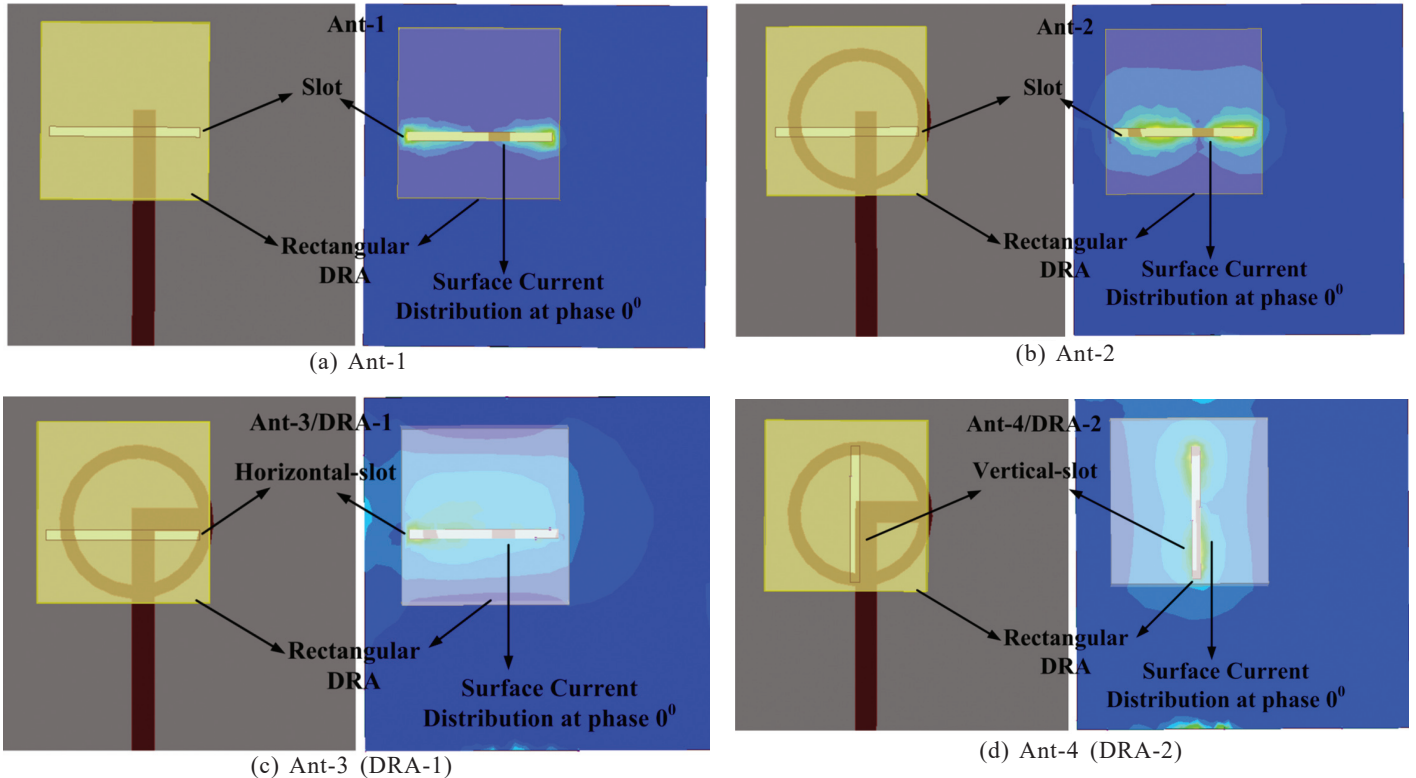
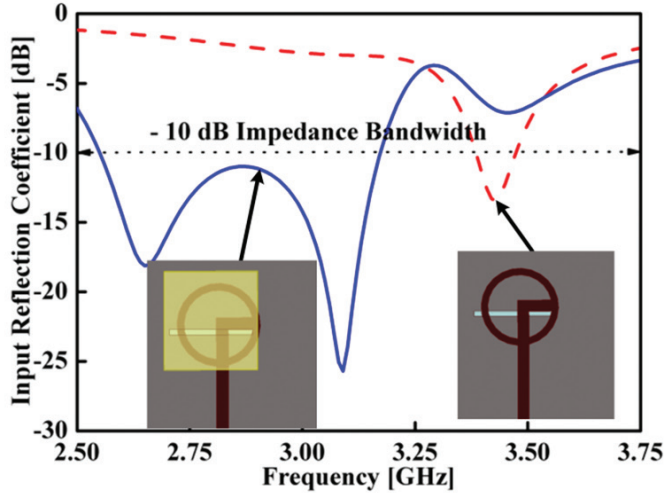
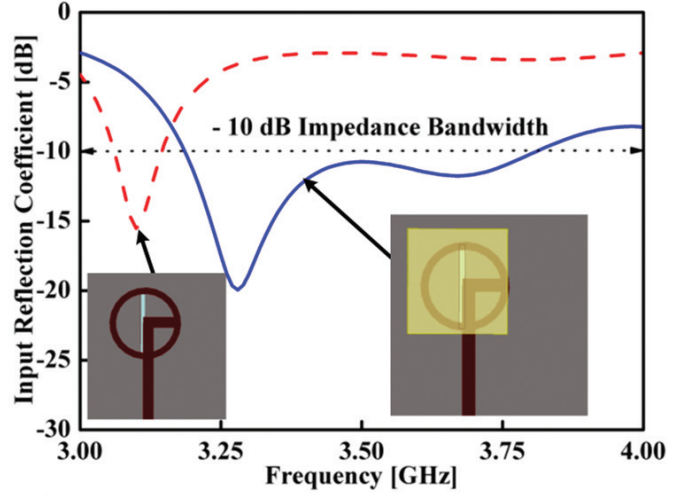


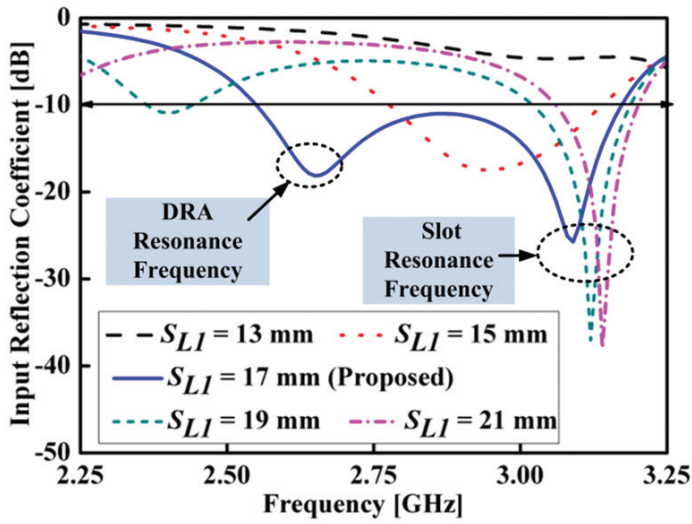
Figure 2. Evolution, surface current distribution and input reflection coefficient of proposed antenna.



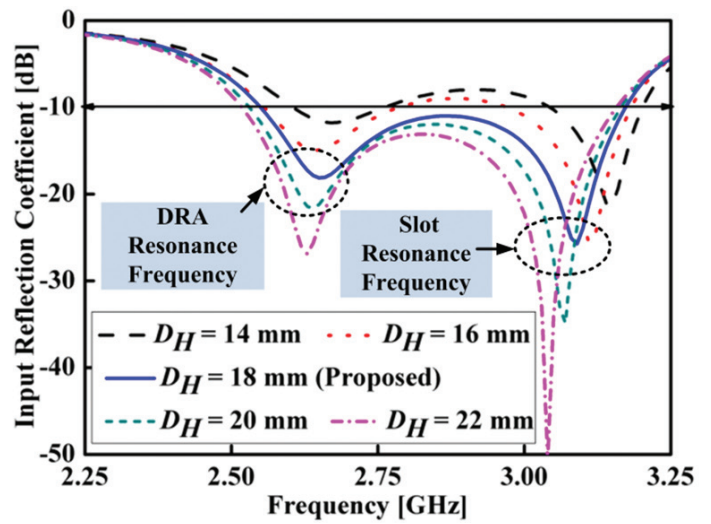
(a) Effect on band of operation due to slot and DR on Ant-3



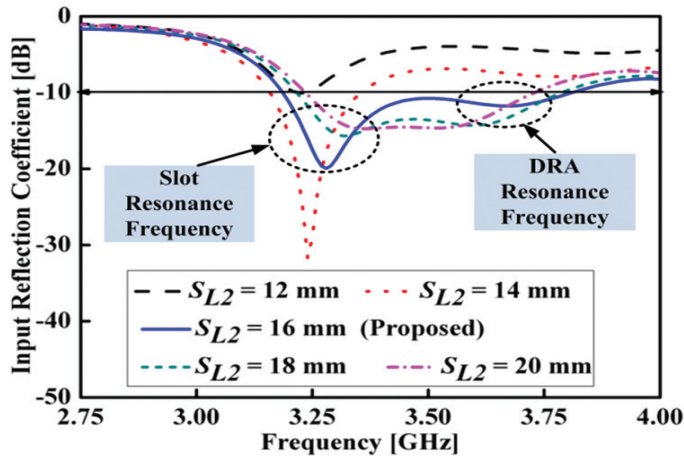
(b) Effect on band of operation due to slot and DR on Ant-4



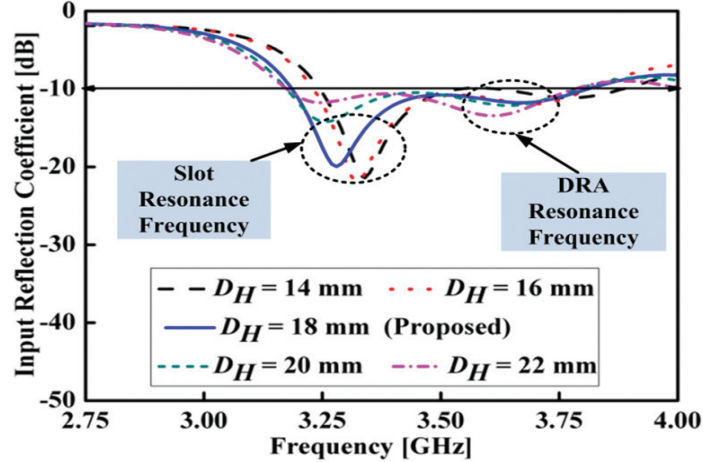
(c) Variation of slot length (DRA-1)



(d) Variation of height of DR (DRA-1)

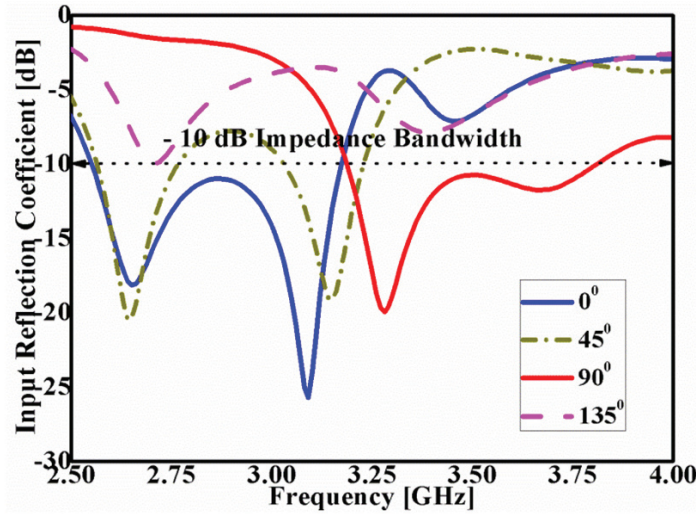


(e) Variation of slot length (DRA-2)



(f) Variation of height of DR (DRA-2)

Figure 3. Effect of various parameters on the proposed DRA-1 and DRA-2.



(g) Frequency tunable performance (mechanical tuning)

Figure 3. Effect of various parameters on the proposed DRA-1 and DRA-2.

Hence the reasonable choice of the slot width is given as follows:

$$S_w = 0.2 \times S_{L1} \text{ or } 0.2 \times S_{L2} \quad (7)$$

$$S_w = 0.2 \times S_{L1} = 0.2 \times 14.57 = 2.91 \text{ mm for DRA-1}$$

$$S_w = 0.2 \times S_{L2} = 0.2 \times 13.71 = 2.74 \text{ mm for DRA-2}$$

- The final part is stub length; the extension of stub is selected so that the reactance must be cancelled out that of the slot aperture. Initially it is chosen as:

$$S_{sub} = \frac{\lambda_g}{4} \quad (8)$$

$$L_{F1} = \frac{\lambda_g}{4} = \frac{36.43}{4} = 9.10 \text{ mm for DRA-1}$$

$$L_{F1} = \frac{\lambda_g}{4} = \frac{34.32}{4} = 8.58 \text{ mm for DRA-2}$$

where, λ_g is the guided wave in the substrate.

$$\lambda_g = \frac{\lambda_0}{\sqrt{\epsilon_{eff} \times \mu_{eff}}} \quad (9)$$

$$\lambda_g = \frac{\lambda_0}{\sqrt{\epsilon_{eff} \times \mu_{eff}}} = \frac{97.08}{\sqrt{7.1 \times 1}} = 36.43 \text{ mm for DRA-1}$$

$$\lambda_g = \frac{\lambda_0}{\sqrt{\epsilon_{eff} \times \mu_{eff}}} = \frac{91.46}{\sqrt{7.1 \times 1}} = 34.32 \text{ mm for DRA-2}$$

After that, we have optimized the slot length ($S_{L1} = 17 \text{ mm}$ and $S_{L2} = 16 \text{ mm}$), slot width ($S_w = 1.1 \text{ mm}$) and stub length ($L_{F1} = 7.35 \text{ mm}$) to obtain the maximum coupling between the DRAs and slots

The final dimensions of DRAs are as follows: $S_{L1} = 17$, $S_{L2} = 16$, $S_w = 40$, $D_L = 20$, $R_2 = 8.5$, $L_{F1} = 7.35$, $D_H = 18$, $S_L = 40$, $S_H = 1.6$, $R_1 = 7$, $S_w = 1.1$, $L_F = 25$, $D_w = 19$, $W_F = 2.5$, which are in mm. For DRA-1 configuration, the horizontal-slot length is taken S_{L1} whereas DRA-2 configuration, the vertical-slot length is taken S_{L2} .

3. PARAMETRIC STUDIES OF DRA-1 AND DRA-2

A parametric study has been concentrated on the optimal performance of feed geometry, effect of resonance frequency

on input reflection coefficient, effect of slot length and height of DR.

3.1 Evolution of Antenna Feed for Frequency Tunable Purpose

Here, the effect of feed geometry on the input reflection factor of DRA-1 and DRA-2 was discussed. To couple the electromagnetic energy properly into the rectangular DR, an efficient shape of feed line has been demonstrated. The evolution of feed line is started from microstrip feed to circular-ring feed and name as Ant-1 to Ant-4, whereas all other antenna parameters are fixed. Here, the HFSS simulation software is used for the simulations purposed of the presented design antenna.

Design procedure of feed line is initiated from simple microstrip feed line named as Ant-1, as shown in Fig. 2(a). But this feed line is not very much suitable to couple the electromagnetic energy with DR, which is also validating by using the surface current distribution as shown in Fig. 2(a). Hence, the result does not show any input impedance bandwidth ($S_{11} < -10 \text{ dB}$), as shown in the Fig. 2(e).

To improve the impedance bandwidth ($S_{11} < -10 \text{ dB}$), a circular ring was added to the existing simple microstrip feed line named Ant-2, as shown in Fig. 2(b). After adding the circular-ring in the feed, the appropriate electromagnetic energy is coupled into the DR, as shown in Fig. 2(b). As a result, this configuration displays 9.19 % (2.60-2.85 GHz) of input impedance bandwidth ($S_{11} < -10 \text{ dB}$) with good impedance matching, as shown in Fig. 2(e). To further improve the input impedance bandwidth ($S_{11} < -10 \text{ dB}$), a stub (L_{F1}) was incorporated to the existing feed line called Ant-3. After the incorporation of the stub in the circular-ring feed line, it was giving the higher coupling of electromagnetic energy into the dielectric resonator and was validated by the distribution of surface current density inside the DRA as shown in Fig. 2(c). This configuration is called DRA-1 (see Fig. 2(c)), and it shows a 21.67 % (2.55-3.17 GHz), input impedance bandwidth, as shown in Fig. 2(e). To obtain frequency tunable application, the DRA-2 configuration has been proposed by

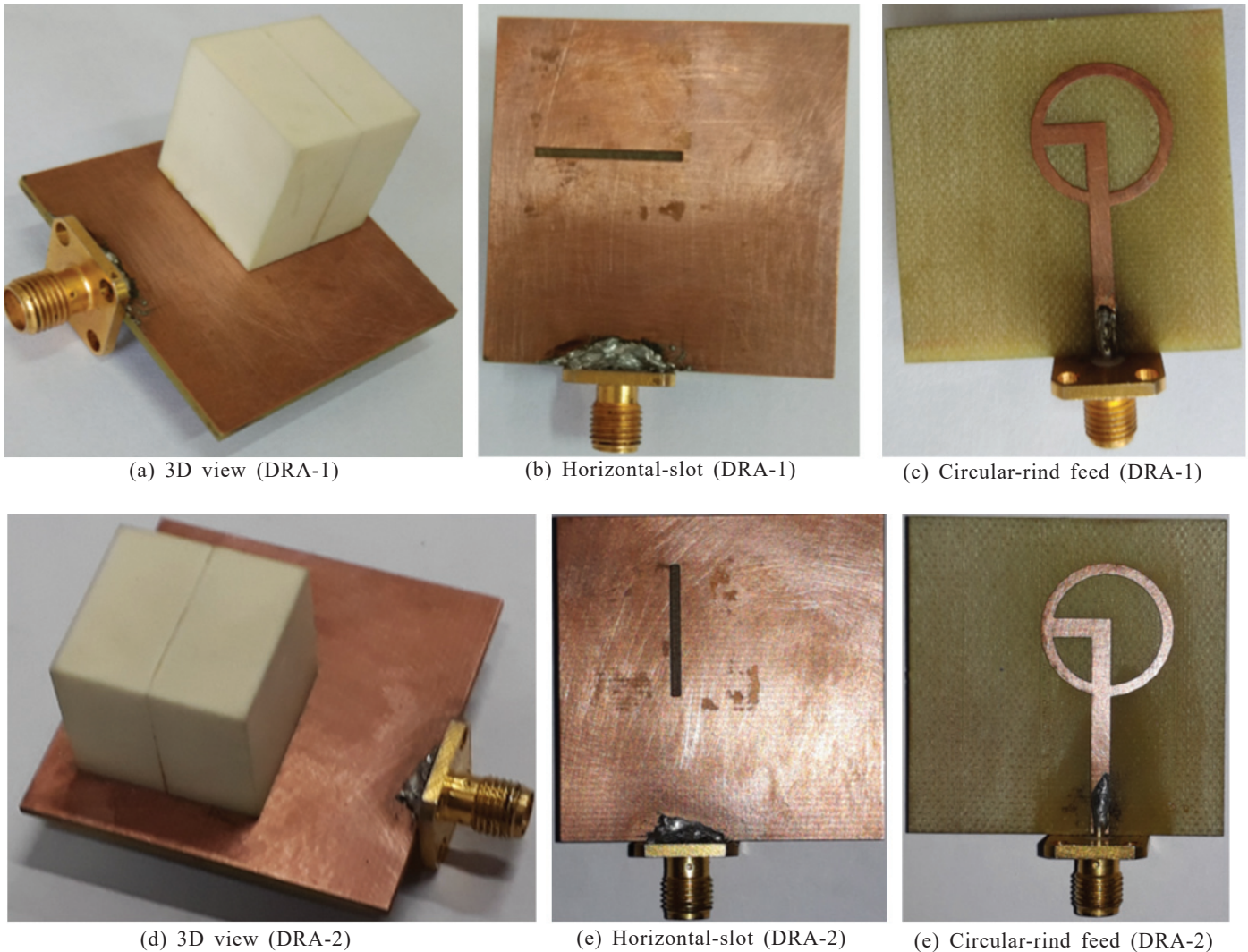


Figure 4. Fabricated photograph of DRA-1 and DRA-2.

changing horizontal-slot into the vertical-slot and remaining all the antenna parameters are fixed, as shown in Fig. 2 (d). The DRA-2 configuration also shows the strong coupling of electromagnetic energy and gives an impedance bandwidth of 18.05 % (3.18-3.81 GHz), which is suitable for Sub-6 GHz/ 5G frequency band applications, as shown in Fig. 2(e).

3.2 Effect on Band of Operation Due to Slot and DR Coupling

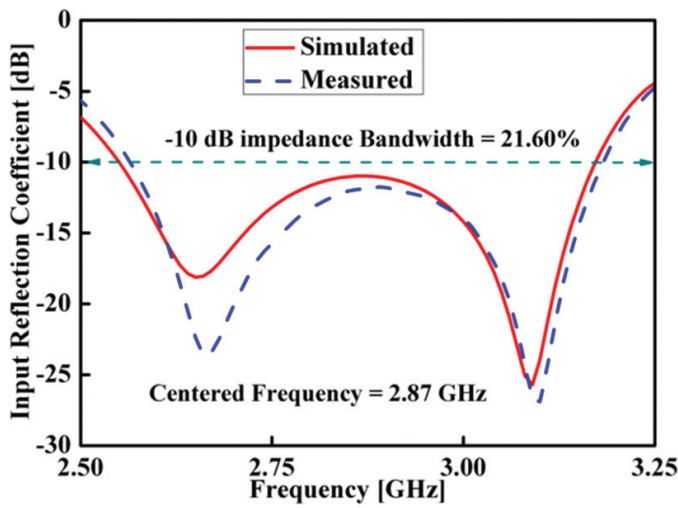
In this sub-section, the effect of slot-circular-ring feed on Ant-3 and slot-circular-ring feed on Ant-3 with DR resonance frequency has been demonstrated. From the literature, DRA and slot both are the resonant structure, if both are combined; it shows dual resonances²⁰. By choosing proper dimensions of DR and slot, the two resonance frequencies have been combined and achieved wide bandwidth. It is clearly observed in DRA-1 configuration from Fig. 3(a-b) that the resonance frequency of slot and DRA are different. By selecting the appropriate dimensions (D_L , D_W , and D_H) of DR and slot (S_{L1} , S_{W1}), the two resonance frequencies i.e., slot and DRA have been merged and achieved wide bandwidth, as shown in Fig. 3(a). In case of DRA-2, the slot and slot with DRA resonance frequency have

been merged and show wide band behaviour of impedance bandwidth, as displayed in Fig. 3(b).

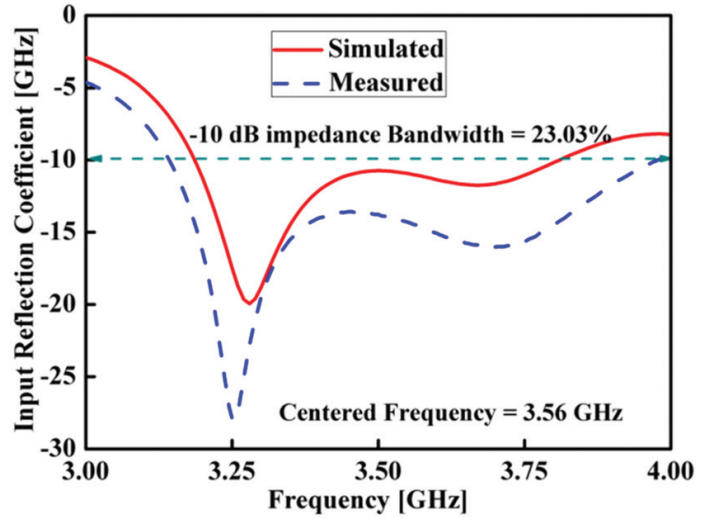
3.3 Effect of Slot Lengths (S_{L1} / S_{L2}) and Height of Dielectric Resonator (DH)

The effect of slot length and DR height on input impedance bandwidth has been explained, as displayed in Figs. 3(c) and (d), respectively. It can be seen from Fig. 3(c), the two resonance frequencies occurred, one is due to the DRA and another one is due to the slot.

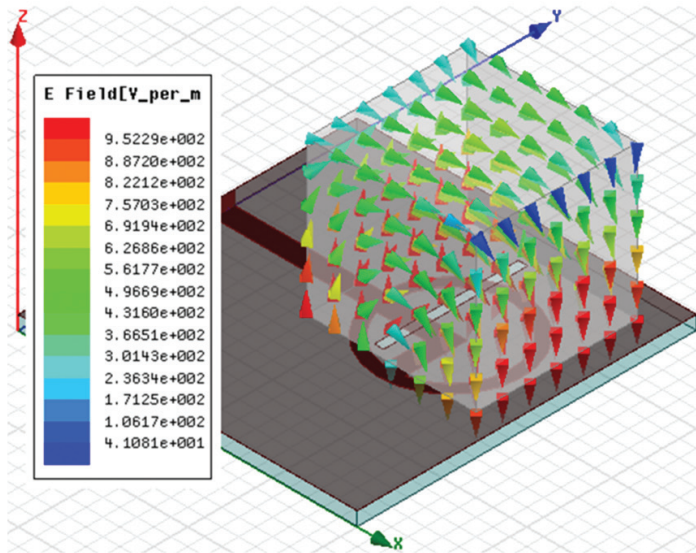
With reference to Fig. 3(c), it can be seen that resonant frequency of DRA and slot are merged, which gives the wideband behaviour of the input impedance bandwidth. These two resonance frequencies are varied by the variation of slot length. But more coupling is occurred on second resonance frequency therefore, it is identify that this is slot resonance frequency. To identify the DRA resonance frequency, height of DR has been varied, as displayed in Fig. 3(d). It can be seen from Fig. 3(d) that first resonance frequency is varied and it is maximum depends on the height of DR, so it is called resonance frequency of DRA.



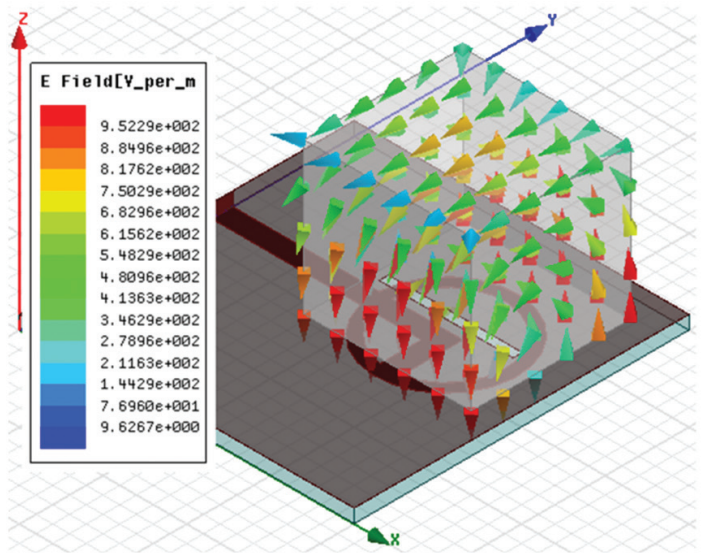
(a) Input reflection coefficient (DRA-1)



(b) Input reflection coefficient (DRA-2)



(c) E-field orientation for DRA-1 at 2.70 GHz



(d) E-field orientation for DRA-2 at 3.70 GHz

Figure 5. Near-field results of proposed DRA-1 and DRA-2.

It can be seen from Fig. 3(e) that variation of slot length is mostly affects the first resonance frequency and show better matching if slot length increases. Therefore, it is confirmed that the first resonance is the slot resonance frequency. To verify the second resonance frequency occurred due to DRA effects only, variation of height of DR has been study. Fig. 3(f) clearly shows that the secondary resonance frequency is primarily affected if the height of the dielectric resonator increases. Therefore, it is confirmed that the second resonance is occurred only due to influence of DRA. Therefore, it is confirmed that the second resonance is occurred only due to influence of DRA.

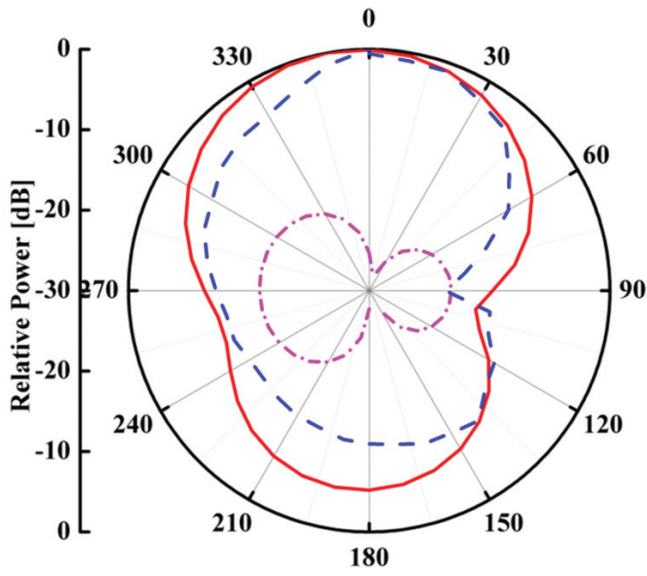
Both the DRA and the slot are radiating structures¹⁸⁻¹⁹ and together they were producing double resonant radiators with identical radiating patterns. If the antenna designers required wide bandwidth behaviours then by selecting the proper design of the DRA and slot; they can merge two resonance frequencies to get wide bandwidth behaviour otherwise it will give two resonances at different frequencies of operations. Positions and size of the slot were modified to enhance the

matching and regulate the resonance frequency using the given Eqns. (5-9). To obtain approximate expressions for individual field components within the dielectric resonator, boundary conditions as well as electric vector potential were used.

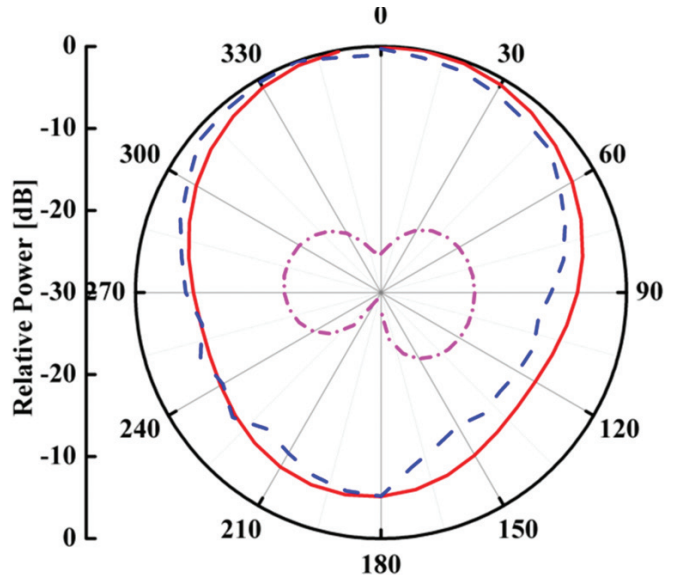
It is worth to mentioning that by varying the slot length and DR height, these two resonance frequencies has been identified and also reported in¹⁸⁻¹⁹.

3.4 Frequency Tunable (Mechanical Tuning)

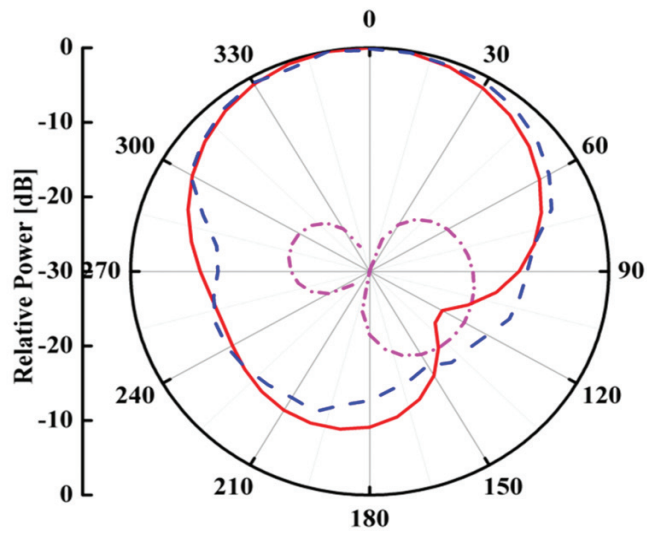
In terms of the frequency tunable performance, the rotation of the slot and its effect on the resonance frequencies is shown in Fig. 3(g). In this proposed work, the tunability is achieved using the mechanical tuning similar to the reported work³³. Here, the rotation of the slot gives the frequency tuning conditions, hence obtained different frequency bands of the applications. It is observed from Fig. 3(g) that the DRA-1 slot act as a reference line, which is nothing but 0° line after that the rotation of the slot is started by taking the step size of 45° i.e., 0° (DRA-1) 45°, 90° (DRA-2) and 135°, respectively for



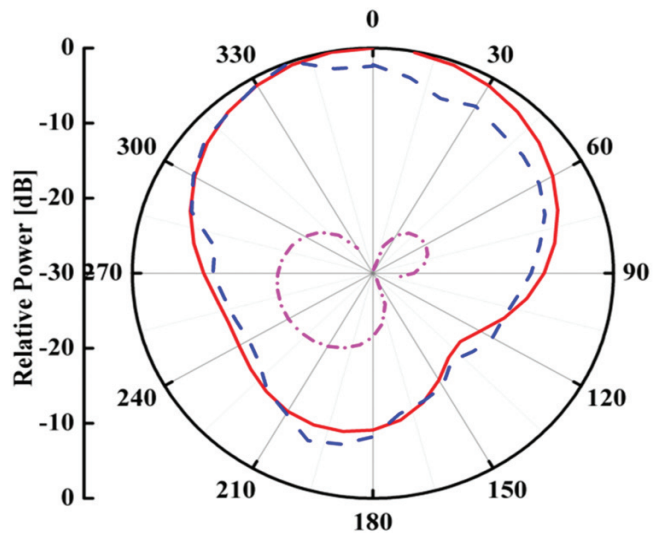
(a) xz -plane at 2.7 GHz (DRA-1)



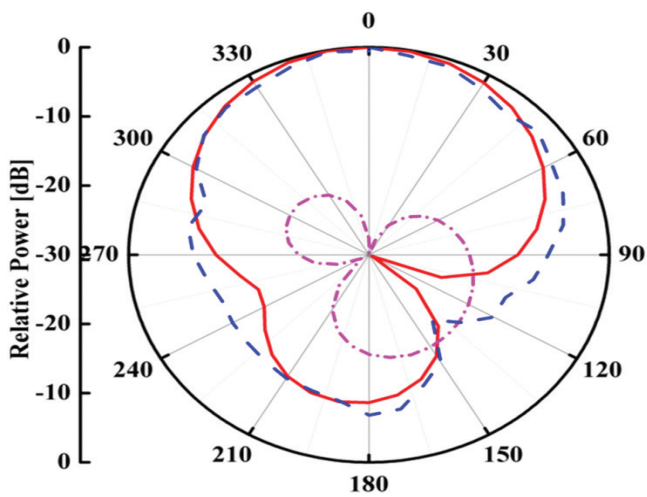
(b) yz -plane at 2.7 GHz (DRA-1)



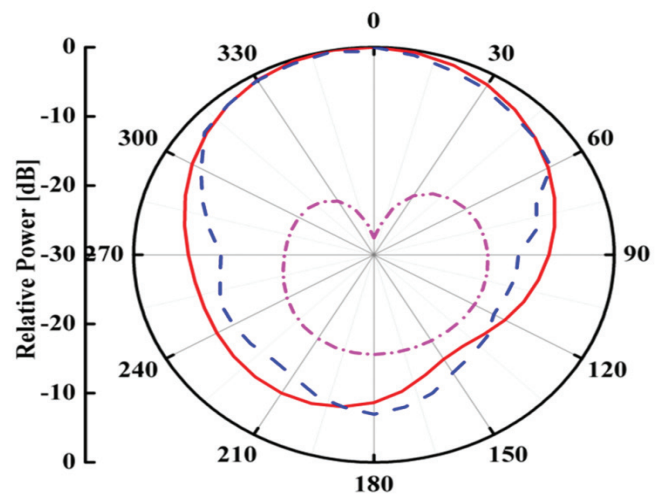
(c) xz -plane at 3.0 GHz (DRA-1)



(d) yz -plane at 3.0 GHz (DRA-1)

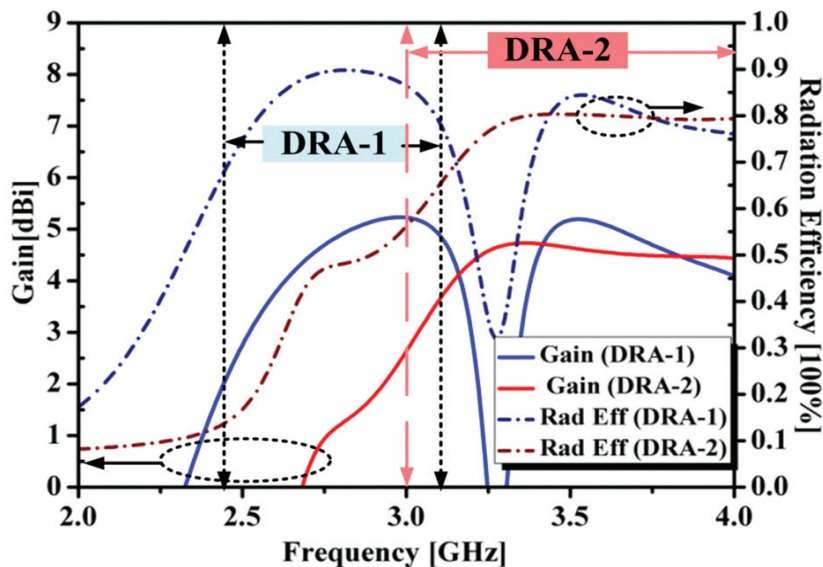
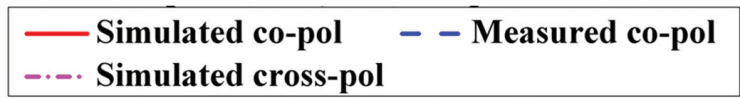
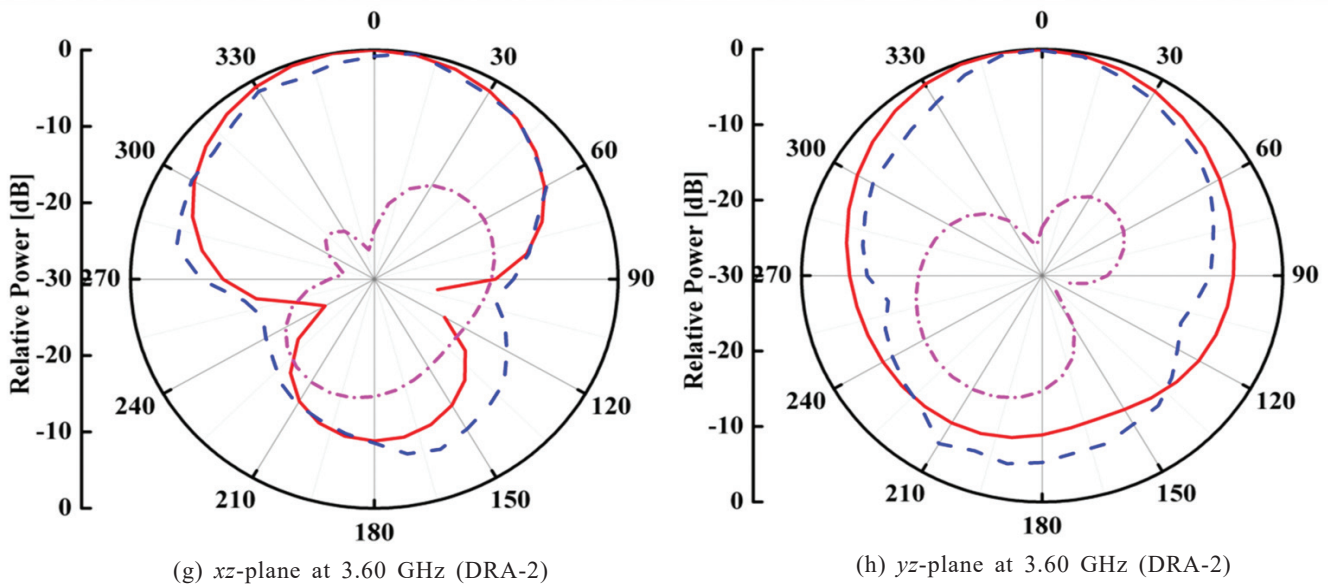


(e) xz -plane at 3.30 GHz (DRA-2)



(f) yz -plane at 3.30 GHz (DRA-2)

Figure 6. Far-field results of proposed DRA-1 and DRA-2.



(i) Total gain and radiation efficiency versus frequency.

Figure 6. Far-field results of proposed DRA-1 and DRA-2.

obtaining the mechanical tuning of the proposed work. It is confirmed that the rotation of the slot is capable for shifting the resonance frequencies and hence shows the frequency tunability condition in the proposed work.

4. RESULT AND DISCUSSIONS

Figure 4 depicts the prototype antenna design of the DRA-1 and DRA-2 configurations. Near and far field results were measured using the PNA network analyser (Keysight N5221A)

Figure 5(a) illustrates the measured and simulated reflection coefficient of proposed DRA-1. Simulated and measured input impedance bandwidth of -10 dB was found to be 21.67 %

(2.55-3.17 GHz) and 21.60 % (2.56-3.18 GHz), respectively. While the simulated and measured input reflection coefficient of DRA-2 is found in Fig. 5(b). For Fig. 5(b), one can see that the simulated and measured input impedance bandwidth of -10 dB was found to be 18.05 % (3.18-3.81 GHz) and 23.03 % (3.15-3.97 GHz), respectively.

The $TE_{11\delta}$ mode was energized in DRA-1 and DRA-2 and confirmed through the field distributions at 2.70 GHz and 3.70 GHz, respectively, as shown in Fig. 5(c) and 5(d). Fig. 6 depicts the simulated and measured standard cross-polarization and co-polarization radiation patterns in two different planes i.e., *xz*- and *yz*-planes of DRA-1 and DRA-2, respectively. For DRA-1 configuration, the co-polarization level is stronger than

Table 1. Comparison of the developed LP DRAs with recently published work

DR Shape	ϵ_r	Feeding mechnisham	DRA mode	Range of BW	% BW ^s	Antenna Size ($\lambda_0 \times \lambda_0$)	Polarisation	Ref.
Cross DRA	9.8	Slot+SMSH	NA [^]	6.07–7.52	21.3	1.08 × 0.96	Linear	8
Rectangular DRA (RDRA)	20	Slot	TE ₁₁₁ / TE ₁₁₂	4.76–5.86	20	0.91 × 0.91	Linear	12
CDRA	35.5	Probe+EBG	HEM ₁₁₆	2.23–2.39	7.0	1.18 × 1.18	Linear	13
Hollow RDRA	10	Conformal strips	TE ₁₁₁	2.24–2.52	11.8	0.98 × 0.98	Linear	14
CDRA	10.2	Slot+metallic cylindar	HEM ₁₁₆	5.4–6.8	23.0	1.8 × 1.8	Linear	15
Hemispherical DRA	14, 20	Slot	NA [^]	2.6-2.7 3.7-3.85	3.77 3.97	2.20 × 2.20	Linear	17
Hemispherical DRA	9.2	Slot	TM ₁₀₁	4.5-5.3	17.58	NA [^]	Linear	18
Cylindrical DRA	10	Conformal strips	HEM ₁₁₆	2.40–2.58	7.2	0.84 × 0.84	Linear	27
Hemispherical DRA	10	Slot	TE ₁₁ / TE ₁₁₂	8.38-8.61 8.94-9.16	2.71/ 2.44	2 × 2	Linear	28
Cylindrical DRA	10	Slot	HEM ₁₁₆	3.8-4.20 7.6-8.4	10/ 10	0.77 × 0.77	Linear	29
RDRA	10	Microstrip-slot	TE ₁₁₁	3.29 - 3.65	10.29	0.57 × 0.57	Linear	30
RDRA	9.8	Slot	TE₁₁₆	2.56–3.18	21.60	0.38 × 0.38	Linear	DRA-1
RDRA	9.8	Slot	TE₁₁₆	3.15-3.97	23.03	0.46 × 0.46	Linear	DRA-2

BW^s = Impedance Bandwidth, NA[^] = Not Available

the cross-polarization level in broadside direction at 2.70 GHz and 3.00 GHz, as shown in Fig. 6(a) and 6(c). It is found that the difference between co-polarization and cross-polarization level showing -24.41 dB at 2.70 GHz and -43.66 dB at 3.00 GHz, respectively. For DRA-2 configuration, the variation between co-polarization and cross-polarization levels is -28.06 dB at 3.30 GHz and -22.88 dB at 3.60 GHz, which is in the direction of broadside, respectively as shown in Fig. 6(e) and 6(g). From the radiation patterns, it is clearly observed that by using the horizontal and vertical slot, the cross-polarization level is reduced down.

The total gain and radiation efficiency were found in Fig. 6(i). It was noted that total gain and radiation efficiency of the presented DRA-1 displays 5.23 dBi and 89.80 %, respectively. Fig. 6(i) shows the total gain and radiation efficiency of the presented DRA-2 and was found to be 4.75 dBi and 79.35 % respectively, in the work band, respectively. The Table 1 provides an in-depth evaluation of the proposed DRA-1 and DRA-2 and earlier reported works. It is clearly found that the proposed work is better than other published work in terms of compactness, ease of fabrication, excitation technique, and basic shape of DR. It also offers wideband behaviour for fundamental mode i.e., TE₁₁₆, and radiates broadside directions. Further, the presented work show frequency tunability, low cross-polarization, better selection of feeding mechanism, and compact size among all the published work which were related to the DRAs.

5. CONCLUSIONS

In this paper, frequency tuneable (mechanical tuning) linearly polarized (TLP) rectangular DRAs have been obtained

by using the horizontal and vertical slot in the same antenna configuration. Here, the resonance frequency of slot and DRA has been identified by using the variation of slot length and height of DR. The proposed linearly polarized antennas have been designed and developed based on the variation of the slot in the ground plane, and was excited by circular-ring feed for applications in broadside directions. Both the proposed LP DRAs are showing TE₁₁₆ mode and are validated by the *E*-field distribution within the rectangular DRA at their resonance frequencies. The DRA-1 and DRA-2 were achieved by using a horizontal slot and a vertical slot in the ground plane. The gain and radiation efficiency of both the proposed DRAs are found to be suitable for different Wi-MAX and Sub-6 GHz 5G frequency band applications.

REFERENCES

- Petosa, A. Dielectric resonator antenna handbook, Norwood, MA, Artech House, Boston, London, UK 2007.
- McAllister, M.W.; Long, S.A. & Conway, G.L. Rectangular dielectric resonator antenna. *IET Electronics Letters*, 1983, **19**(6), 218-219. doi:10.1049/el:19830150
- Kajfez, D.A.; Glisson, W. & James, J. Computed modal field distributions for isolated dielectric resonators. *IEEE Trans. Micro. Theory Technol.*, 1984, **32**(12), 1609-1616. doi: 10.1109/TMTT.1984.1132900
- Mongia, R.K. & Bhartia, P. Dielectric resonator antennas-a review and general design relations for resonant frequency

- and bandwidth. *Int. J. Microw. Millimeter-Wave Comput.-Aided Eng.*, 1994, **4**(3), 230-247.
doi: 10.1002/mmce.4570040304.
5. Mongia, R.K. & Ittipiboon, A. Theoretical and experimental investigations on rectangular dielectric resonator antennas. *IEEE Trans. Antennas Propag.*, 1997, **45**(9), 1348–1356.
doi: 10.1109/8.623123
 6. Luk, K.M. & Leung, K.W. Dielectric resonator antenna, Research Studies Press Ltd, England, 2003.
 7. Chaudhary, R.K.; Kumar, R. & Chowdhury, R. Circularly polarised dielectric resonator antennas, Artech House, Boston, London, UK 2021.
 8. Chaudhary, R.K.; Kumar, R. & Srivastava, K.V. Wideband ring dielectric resonator antenna with annular-shaped microstrip feed. *IEEE Antennas Wirel. Propag. Lett.*, 2013, **12**, 595–598.
doi: 10.1109/LAWP.2013.2260317
 9. Sullivan, P.L. & Schaubert, D.H. Analysis of an aperture coupled microstrip antenna. *IEEE Trans. Antennas Propag.*, 1986, **34**(8), 977–984.
doi: 10.1109/TAP.1986.1143929
 10. Leung, K.W.; Luk, K.M.; Lai, K.Y.A. & Lin, D. Theory and experiment of an aperture-coupled hemispherical dielectric resonator antenna. *IEEE Trans. Antennas Propag.*, 1995, **43**(11), 1192–1198.
doi: 10.1109/TAP.2004.842681
 11. Pozar, D.M. Microwave Engineering. 2nd ed. New York, NY, USA: Wiley, 1998.
 12. Kishk, A.A. Wide-band truncated tetrahedron dielectric resonator antenna excited by a coaxial probe. *IEEE Trans. Antennas Propag.*, 2003, **51**(10), 2913–2917.
doi: 10.1109/TAP.2003.816300
 13. Chair, R.; Kishk, A.A. & Lee, K.F. Experimental investigation for wideband perforated dielectric resonator antenna. *Electr. Lett.*, 2006, **42**(3), 137–139.
doi: 10.1049/el:20063987
 14. Nasimuddin, N. & Esselle, K.P. A low-profile compact microwave antenna with high gain and wide bandwidth. *IEEE Trans. Antennas Propag.*, 2007, **55**(6), 1880–1883.
doi: 10.1109/TAP.2007.898644
 15. Chaudhary, R.K.; Srivastava, K.V. & Biswas, A. A broadband dumbbell-shaped dielectric resonator antenna. *Microw. Opt. Technol. Lett.*, 2014, **56**(12), 2944–2947.
doi: 10.1002/mop.28743
 16. Mukherjee, B.; Patel, P. & Mukherjee, J. Hemispherical dielectric resonator antenna based on apollonian gasket of circles-A fractal approach. *IEEE Trans. Antennas Propag.*, 2014, **62**(1), 40–47.
doi: 10.1109/TAP.2013.2287011
 17. Gupta, R.D. & Parihar, M.S. Investigation of an asymmetrical E-shaped dielectric resonator antenna with wideband characteristics. *IET Microwaves, Antennas Propag.*, 2016, **10**(12), 1292–1297.
doi: 10.1049/iet-map.2016.0167
 18. Buerkle, A.; Sarabandi, K. & Mosallaei, H. Compact slot and dielectric resonator antenna with dual-resonance, broadband characteristics. *IEEE Trans. Antennas Propag.*, 2005, **53**(3), 1020–1027.
doi: 10.1109/TAP.2004.842681
 19. Majeed, A.H.; Abdullah, A.S.; Elmegri, F.; Sayidmarie, K.H.; Abd-Alhameed, R.A. & Noras, J.M. Aperture coupled asymmetric dielectric resonators antenna for wideband applications. *IEEE Antennas Wirel. Propag. Lett.*, 2014, **13**, 927–930.
doi: 10.1109/LAWP.2014.2322779
 20. Chang, T.H.; Huang, Y.C.; Su, W.F. & Kiang, J.F. Wideband dielectric resonator antenna with a tunnel. *IEEE Antennas Wirel. Propag. Lett.*, 2008, **7**, 275–278.
doi: 10.1109/LAWP.2008.928477
 21. Denidni, T.A.; Coulibaly, Y. & Boutayeb, H. Hybrid dielectric resonator antenna with circular mushroom-like structure for gain improvement. *IEEE Trans. Antennas Propag.*, 2009, **57**(4), 1043–1049.
doi: 10.1109/TAP.2009.2015809
 22. Fang, X.S.; Leung, K.W.; Lim, E.H. & Chen, R.S. Compact differential rectangular dielectric resonator antenna. *IEEE Antennas Wirel. Propag. Lett.*, 2010, **9**, 662–665.
doi: 10.1109/LAWP.2010.2057402
 23. Wang, Y.F.; Denidni, T.A.; Zeng, Q.S. & Wei, G. Design of high gain, broadband cylindrical dielectric resonator antenna. *Electr. Lett.*, 2013, **49**(24), 1506–1507.
doi: 10.1049/el.2013.2741
 24. Kumar, R. & Chaudhary, R.K. Circularly polarised rectangular DRA coupled through orthogonal slot excited with microstrip circular ring feeding structure for Wi-MAX Applications. *Int. J. RF Microw Comput Aided Eng.*, 2017, **28**(1), 1–7.
doi: 10.1002/mmce.21153
 25. Hosseinbeig, A.; Kamyab, M. & Meiguni, J.S. Theory of aperture-coupled hemispherical dielectric resonator antennas with radiating elements. *Int. J. Electron. Commun.*, 2013, **67**(11), 975–980.
doi: 10.1016/j.aeue.2013.05.010
 26. Mukherjee, B. A novel half hemispherical dielectric resonator antenna with array of slots loaded with a circular metallic patch for wireless applications. *Int. J. Electron. Commun.*, 2015, **69**(12), 1755–1759.
doi: 10.1016/j.aeue.2015.08.012
 27. Liu, Y.T.; Leung, K.W.; Ren, J. & Sun, Y. X. Linearly and circularly polarized filtering dielectric resonator antennas. *IEEE Trans. Antennas Propag.*, 2019, **67**(6), 3629 - 3640.
doi: 10.1109/TAP.2019.2902670
 28. Ghosh, B.; Bhattacharya, D.; Sinha, P.D. & Werner, D. H. Design of Circular Waveguide Annular Slot-Coupled Two-Layer DRA for Linear and Circular Polarizations. *IEEE Antennas Wireless Propag. Lett.*, 2020, **19**(6), 1012-1016.
doi: 10.1109/LAWP.2020.2986375
 29. Gupta, P.; Guha, D. & Kumar C. Dual-mode cylindrical DRA: Simplified design with improved radiation and bandwidth. *IEEE Antennas Wireless Propag. Lett.*, 2021, **20**(12), 2359-2362.
doi: 10.1109/LAWP.2021.3110875
 30. Wang, C.; Zhang, Y.; Han, Z.; Chen, G.; Guan, X. &

- Ren, B. A novel single-feed filtering dielectric resonator antenna using slotline-loaded coupling structure. *Micro. Opt. Technol. Lett.*, 2022, **64**(4), 750-754, doi: 10.1002/mop.33164.
31. Petosa, A. An overview of tuning techniques for frequency-agile antennas. *IEEE Antennas Propag. Mag.*, 2012, **54**(5), 271–296. doi: 10.1109/MAP.2012.6348178
 32. Ng, H.K. & Leung, K.W. Frequency tuning of the linearly and circularly polarized dielectric resonator antennas using multiple parasitic strips. *IEEE Trans. Antennas Propag.*, 2006, **54**(1), 225-230. doi: 10.1109/TAP.2005.861546
 33. Tan, L.R.; Wu, R.X.; Wang, C.Y. & Poo, Y. Ferrite-loaded SIW bowtie slot antenna with broadband frequency tunability. *IEEE Antennas Wireless Propag. Lett.*, 2014, **13**, 325-328. doi: 10.1109/LAWP.2014.2305431.
 34. Singh, A. & Saavedra, C.E. Fluidic stub-loaded patch antenna for frequency-tunable polarization reconfiguration. *IEEE Open J. Antennas Propag.*, 2021, **2**, 362-369. doi: 10.1109/OJAP.2021.3063281.
 35. Wu, Y.; Vallecchi, A.; Yang, Y.; You, Z.; Shamonina, E.; Stevens, C.J. & Grant, P.S. 3D printed active origami dielectrics for frequency tunable antennas through mechanical actuation. *IEEE Access*, 2022, **10**, 103552-103562. doi: 10.1109/ACCESS.2022.3197178.

CONTRIBUTORS

Dr Rajkishor Kumar obtained his PhD from the Department of Electronics Engineering at Indian Institute of Technology (Indian School of Mines) Dhanbad, India and he is working as an Assistant Professor Senior Grade at the School of Electronics Engineering in the Department of Communication Engineering, Vellore Institute of Technology, Vellore, Tamil Nadu, India. He has contributed in terms of simulation, fabrication, measurements, and manuscript writing.

Dr Avinash Chandra obtained his Ph.D. in Electronics and Communication with specialisation in RF/Microwave engineering from IIT-Dhanbad and he is working as an Associate Professor in the school of Electronics Engineering, Vellore Institute of Technology, Vellore, Tamil Nadu, India. His current research area is of waveguides, reconfigurable arrays, Antennas, for 6G Applications. He has contributed to the parametric study of antenna design.

Dr Naveen Mishra obtained his PhD degree from the Department of Electronics Engineering, IIT (Indian School of Mines) Dhanbad, India. He is working as an Assistant Professor with the Department of Electronics Engineering, School of Electronics Engineering, Vellore Institute of Technology, Vellore, Tamilnadu, India. He has contributed to the parametric study of antenna design.

Dr Raghvendra Kumar Chaudhary is an Associate Professor at the Department of Electrical Engineering, IIT, Kanpur, India. His current research area is Reconfigurable Metamaterial for Compact Antenna design, MIMO and Cognitive Radio Antenna and multifunctional Filter, mmWave Devices, Frequency Reconfigurable Active Array Antenna with Beam Steering, Circularly Polarized Dielectric Resonator Antenna and Metasurface structures. He has contributed as a guide.